JOURNAL OF MATERIALS SCIENCE 32 (1997) 1357–1363

Subsolidus phase relationships in the ZrO_2-rich part of the ZrO_2–Zr_3N_4 system

M. LERCH, O. RAHÄUSER
Silicatchemie, Universität Würzburg, Germany

Zirconia can be stabilized by incorporation of nitrogen. The phase relationships in the ZrO_2-rich part of the system ZrO_2–Zr_3N_4 have been investigated using high-temperature X-ray methods. At temperatures above 1000 °C, a tetragonal and a cubic phase with randomly distributed vacancies exists, depending on the amount of incorporated nitrogen. This high-temperature behaviour is similar to that of systems like ZrO_2–Y_2O_3, which is another indication for the important role of anion vacancies in zirconia systems. Below 1000 °C, β-type phases with an ordered arrangement of anion vacancies are stable.

1. Introduction

ZrO_2 exists in three solid polymorphs at atmospheric pressure. It is monoclinic at ambient temperature, tetragonal in a temperature range between ~1175 and ~2400 °C, and cubic up to the melting point of nearly 2700 °C. It is possible to stabilize the high-temperature polymorphs at ambient temperature by doping the ZrO_2 with aliovalent oxides like Y_2O_3, MgO, or CaO. Many authors have investigated the systems ZrO_2–Y_2O_3, ZrO_2–MgO, and ZrO_2–CaO (e.g. [1–8]) and the phase relationships can be considered as well-known. The ZrO_2-rich part of these systems is of interest, because the cubic and tetragonal phases are important for technical applications like fuel cells, oxygen sensors, refractories, etc. Doping with aliovalent oxides leads to the formation of oxygen vacancies because of charge neutrality. Anion vacancies are an important factor for the outstanding ionic conductivity of zirconia ceramics.

A new approach, which has received far less attention both in research and application in the past, is the doping with aliovalent anions. The following defect equation describes the formation of anion vacancies due to incorporation of nitrogen into ZrO_2

$$3O_O^x + N_2 = 2N_O' + V_O^{\circ\circ} + \tfrac{3}{2}O_2 \qquad (1)$$

First studies of the system Zr–O–N were made by Gilles *et al.* [9, 10]. They reported three oxynitride phases (γ, β, β′), which are derived from the fluorite structure of cubic zirconia. Cheng and Thompson [11, 12] found another Zr–O–N phase called β″. The results of our recent studies [13, 14] are summarized below, together with the composition of the compounds.

$Zr_7O_{11}N_2$	β′ phase	(21 mol % $ZrN_{4/3}$)
$\sim Zr_7O_{9.5}N_{3.0}$	β″ phase	(~34 mol % $ZrN_{4/3}$)
$Zr_7O_8N_4$	β phase	(43 mol % $ZrN_{4/3}$)
Zr_2ON_2	γ phase	(75 mol % $ZrN_{4/3}$)

All these zirconium oxynitride phases belong to the system ZrO_2–Zr_3N_4 and can be described by the general formula $ZrO_{2-2x}N_{4x/3}$. Direct nitridation of ZrO_2 in a nitrogen atmosphere (graphite-heated resistance furnace) at temperatures above 1400 °C leads to β′ or β″ phase (β-type phases). γ and β phases were synthesized by reaction of ZrO_2/ZrN mixtures with NH_3 [9, 10] at 1000 °C. Another way is the reaction of $ZrCl_4$ with NH_3 and oxygen [15]. In contrast to cation-stabilized zirconia (randomly distributed vacancies), however, the anion vacancies in nitrogen-stabilized zirconia show an ordered arrangement. In β-type phases (trigonal), vacancies are ordered along one of the former cubic three-fold axes which becomes the trigonal *c*-axis. Structural details are described elsewhere [14–16].

The ZrO_2-rich part of the system ZrO_2–Zr_3N_4 may be an interesting field for phases with good ionic conductivity. Almost nothing is known about the high-temperature behaviour of β-type phases. The aim of this work was to investigate this behaviour for compositions of up to nearly 25 mol % $ZrN_{4/3}$ using high-temperature X-ray powder methods. It is possible to prepare such samples by direct nitridation of ZrO_2. Zirconia with various amounts of nitrogen can be synthesized by variation of, for example, the temperature of nitridation.

2. Experimental procedure

β″/m-ZrO_2 mixtures were prepared by nitridation of a commercial ZrO_2 powder (Alpha) in a graphite-heated resistance furnace (KCE) in a nitrogen atmosphere of 1 bar. Temperatures between 1400 and 1900 °C and a nitridation time of 2 h were used. Before the heat treatment, the powder was isostatically pressed into pellets (KIP 200E, Weber). The pellets were powdered and homogenized after nitridation.

High-temperature X-ray powder investigations between ambient temperature and 1200 °C were carried

0022–2461 © 1997 Chapman & Hall

out using a STOE STADIP diffractometer (Debye Scherrer geometry, $CuK_{\alpha1}$ radiation, $\lambda = 0.15406$ nm, position sensitive detector) with a graphite heated furnace. Owing to their poor oxidation resistance at temperatures above 600 °C [13], the powders were filled into capillaries under nitrogen. The samples were heated at a rate of $20\,^{\circ}C\,min^{-1}$. When a given temperature was reached, diffraction data were collected for 15 min after an annealing time of 15 min. Longer dwell periods did not lead to significantly different results.

A vertical furnace (LORA 20/19, Reetz and Partner) was used for quenching experiments. The samples, embedded in graphite, were quenched from 1400 °C into water, in a nitrogen atmosphere.

N/O analysis of the samples was performed using the method of hot-gas extraction (Leco).

3. Results and discussion

In order to obtain information about phase relationships in the ZrO_2-rich part of the ZrO_2–Zr_3N_4 system, several samples with different amounts of nitrogen were prepared by direct nitridation of ZrO_2. Variation of the temperature between 1400 and 1900 °C led to the formation of β''/m-ZrO_2 samples consisting of 5 wt %–71 wt % β'' ($Zr_7O_{0.95}N_{3.0}$) after furnace cooling (3 h to ambient temperature). A detailed study of the β'' content as a function of parameters like temperature, nitridation time, and nitrogen pressure is presented elsewhere [13, 17].

The total nitrogen content of the samples was determined by two methods. One route was chemical analysis using the method of hot-gas extraction. For high nitridation temperatures, the formation of ZrN was observed. The main disadvantage with the extraction method is that it is impossible to distinguish between nitrogen from ZrN and β''. However, a significant amount of ZrN was detected only for samples with a β'' content of more than 50 wt %. The second route was quantitative analysis of X-ray powder data using the polymorph method described by Garvie and Nicholson [18]. They calculated the content of monoclinic phase (wt %) with the following equation.

$$x_m = \frac{I_m(1\,1\,1) + I_m(1\,1\,\bar{1})}{I_m(1\,1\,1) + I_m(1\,1\,\bar{1}) + I_c(1\,1\,1)}, \quad (2a)$$

$$x_{\beta''} \sim x_c = 1 - x_m \quad (2b)$$

I_m and I_c represent the intensities of the strongest reflections of monoclinic and cubic zirconia, respectively; the β'' phase was treated as cubic for the calculations. This allows the nitrogen content due to β'' to be determined, even if ZrN is present. Electron energy loss spectroscopy (EELS) investigations have shown that no detectable amount of nitrogen is dissolved in monoclinic ZrO_2 at ambient temperature [13]. It should be mentioned that ZrN is not involved in the high-temperature reaction in the investigated field of composition.

Fig. 1a shows an X-ray powder diagram of a β''/m-ZrO_2 sample. The reflections of the β'' phase are very similar to that of cubic zirconia, and it is very difficult to distinguish between them. Very small additional superlattice reflections could be observed for β''. This is shown in Fig. 1b, where the region of small angles is presented in detail. A measuring time of 24 h and the use of a position sensitive detector is necessary to distinguish between β'' and cubic zirconia or the other β-type phases. The intensities of the superlattice reflections are in the order of 1/1000 of the strongest reflection. Thus, it is not possible to observe these reflections in common high-temperature measurements. For refinements of lattice parameters, the β'' phase was treated as cubic in this case.

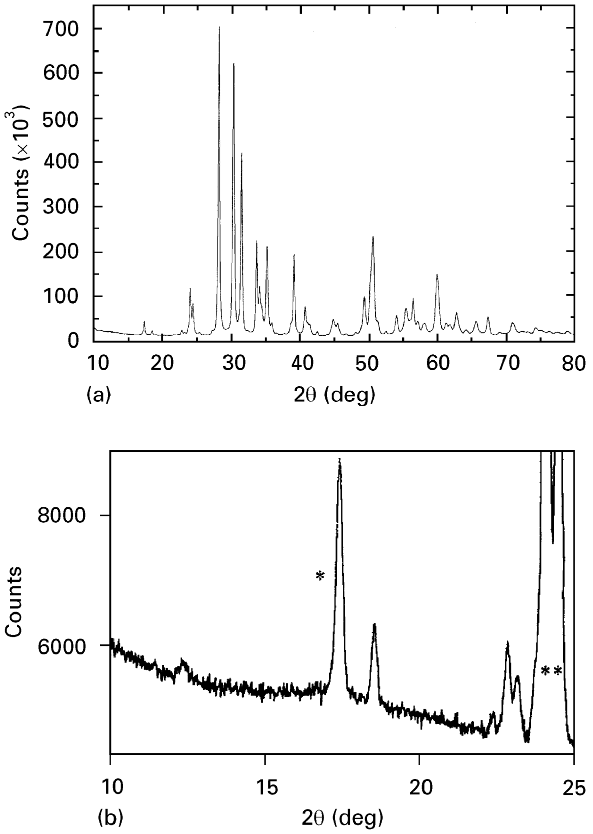

Figure 1 (a) X-ray powder diagram of a β''/m-ZrO_2 sample. (b) The small-angle region in more detail. Monoclinic reflections are marked.

The results of high-temperature X-ray investigations of two β''/m-ZrO_2 samples containing 25 and 71 wt % β'' phase, respectively, are presented in Fig. 2a and b. The 2θ range between 27° and 36° is shown, because reflections in this region are very strong and also instructive for phase analysis.

The diagram shown in Fig. 2a is dominated by the reflections of monoclinic ZrO_2 (75 wt %). At temperatures of ~1000 °C, the intensity of the reflections of the monoclinic phase decreases and a tetragonal phase can be observed. Thus, the reflection at nearly 35° is split.

A different behaviour was observed for the sample containing only 29 wt % monoclinic ZrO_2. Again, the intensity of the reflections of monoclinic ZrO_2 decreases at ~1000 °C. In contrast to the sample consisting of 75 wt % monoclinic phase, only a cubic high-temperature phase was detected. It should be noted that there is a significant amount of ZrN in this

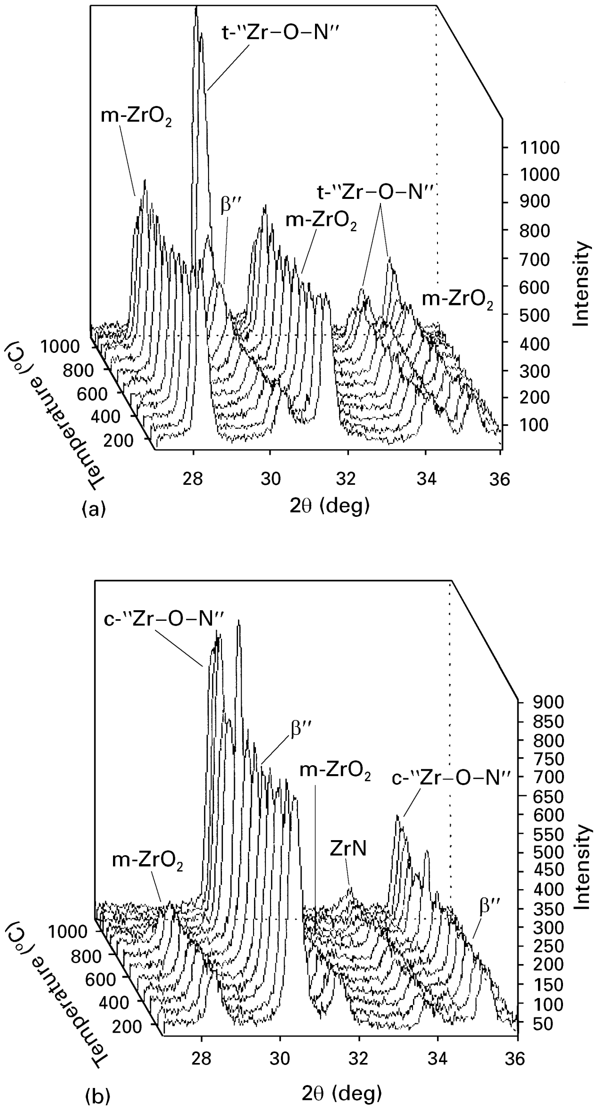

Figure 2 High-temperature X-ray powder diagrams of β''/m-ZrO_2 samples with (a) 25 wt % and (b) 71 wt % β'' (at ambient temperature) as starting composition.

sample. Its content is still the same before and after heating. ZrN is not involved in the phase transition.

The usual mixture of β''/m-ZrO_2 was observed after cooling the samples to ambient temperature. At nearly 1000 °C, the high-temperature phases decompose to β'' and m-ZrO_2. In order to gain information about order–disorder processes, high-temperature neutron scattering investigations were carried out (HRPD, RAL, UK). There is no indication of ordered vacancies in the high-temperature phases [19].

Further investigations were carried out with β''/m-ZrO_2 samples in the range 5–71 wt % β''. In Fig. 3, the phase relationships, determined by high-temperature X-ray methods, are presented. The β'' phase with ordered anion vacancies is stable up to a temperature of nearly 1000 °C. At temperatures above this, a tetragonal or cubic high-temperature phase with randomly distributed vacancies exists, depending on the content of incorporated nitrogen. The coexistence field of tetragonal and cubic was determined by intensity analysis of the reflections. It should be noted that there is no real certainty of equilibrium, especially at lower temperatures. No reliable temperature-dependent data on the solubility of nitrogen in monoclinic ZrO_2 are available. Its solubility is $<0.2\%$ at ambient temperature [13]. Neglecting the ordered vacancies at low temperatures, the phase relationships are similar to that in the systems ZrO_2–Y_2O_3, ZrO_2–CaO, or ZrO_2–MgO. This is evident, because the existence of anion vacancies seems to be one of the main determinants for the phase relationships; the reason for formation (doping with aliovalent cations or anions) is not an important factor.

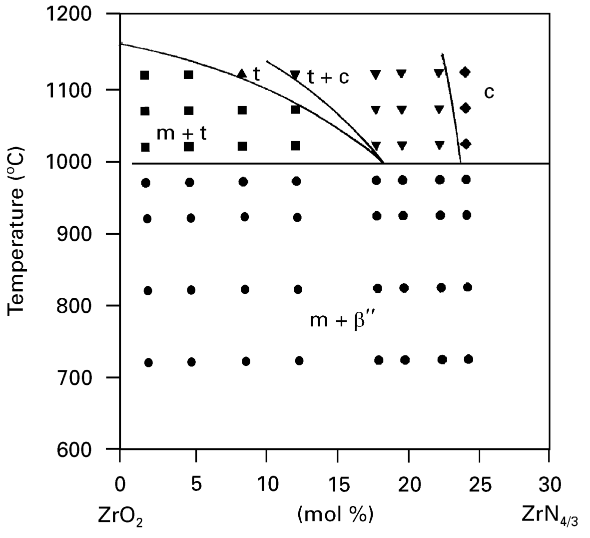

Figure 3 Subsolidus phase relationships in the ZrO_2-rich part in the ZrO_2–$ZrN_{4/3}$ system.

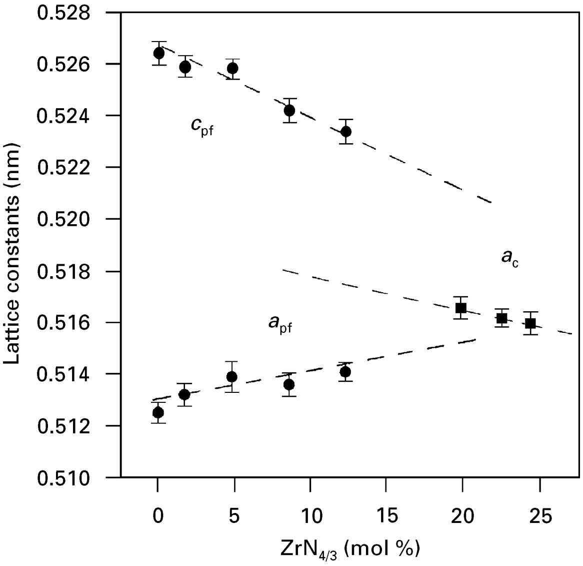

Figure 4 Lattice parameters of the cubic (a_c) and tetragonal (pseudofluorite setting: a_{pf}, c_{pf}) high-temperature phases for a temperature of 1120 °C.

The refined lattice constants at 1120 °C are shown in Fig. 4. A pseudofluorite setting is presented for the tetragonal cell, because comparison between the cubic and tetragonal cell is easier in this case. Pseudofluorite lattice parameters of the tetragonal cell (a_{pf}, c_{pf}) were calculated from $a_{pf} = 2^{1/2}a_t$ and by $c_{pf} = c_t$, respectively (a_t and c_t are the lattice parameters of the commonly used smaller unit cell). In the coexistence field of tetragonal and cubic, lattice parameters could be refined seriously only for the dominating phase. The length of the tetragonal *a*-axis increases while the *c*-axis decreases, however, with an increasing content of $ZrN_{4/3}$. The cubic lattice constant decreases with increasing content of the nitride. The behaviour of the tetragonal phase is very similar to the reported results for, for example, the system ZrO_2–Y_2O_3 [20], which is another indication of the important role of anion vacancies in zirconia systems. With increasing concentration of anion vacancies, which is equivalent to an increasing concentration of $ZrN_{4/3}$, the cell volume decreases.

As an example, the lattice parameter of a sample containing 35% β″ ZrO_2 (at ambient temperature) as a function of temperature is presented in Fig. 5. A sample with a high nitrogen content was selected, because of the strong intensities of β″ reflections. The high-temperature phase and β″ were indexed cubic. Approximately three regions of thermal behaviour can be distinguished. First, a region above the phase transition between ~1000 and 1170 °C, where the thermal expansion was linear with an expansion coefficient of $\alpha = 13 \times 10^{-6}\ K^{-1}$. With decreasing temperature, the lattice parameter decreases anomalously between 1000 and 800 °C. Below this region, the thermal expansion coefficient reaches a value of $12 \times 10^{-6}\ K^{-1}$ (~600–800 °C), which is very similar to that of the high-temperature phase. However, there is a simple explanation for the non-linear behaviour in the region between ~ 800 and 1000 °C. As described above, the cell constant of the nitrogen-stabilized phase decreases with increasing nitrogen content. β″ ($Zr_7O_{9.5}N_{3.0}$) reacts with ZrO_2 to give a high-temperature phase containing nitrogen. For a content of 35 wt % m-ZrO_2 (ambient temperature), the composition of the high-temperature phase is ~ $Zr_7O_{11.1}N_{2.0}$. This decreased nitrogen content leads to the anomalous increase of the lattice parameter. It should be noted that the determined coefficients of thermal expansion above and below the phase transition are very similar to the coefficients given for, for example, yttria-stabilized cubic zirconia ($\alpha = 11 \times 10^{-6}\ K^{-1}$ [21]). This is a further point showing the similarities between zirconia stabilized with oxides or nitrogen.

As described above, the high-temperature phases decompose into β″ and monoclinic ZrO_2 during furnace cooling to ambient temperature. This reaction of a homogeneous, nitrogen-containing phase to a phase with a higher nitrogen content (β″) and a compound without nitrogen (m-ZrO_2) is controlled by diffusion of the oxygen and nitrogen ions. Fig. 6a shows a scanning electron micrograph of the microstructure of a β″/m-ZrO_2 sample. The pellet was etched in HF (38%) for 20 min. It consists of needles (m-ZrO_2) embedded in a matrix of β″. Because of the diffusive and non-martensitic character of this reaction, the cooling rate seems to be an important factor in the formation of low-temperature phases. Such a β″/m-ZrO_2 pellet was reheated in a vertical furnace up to 1400 °C and then quenched into water. Fig. 6b shows smaller needles than the slowly cooled sample because there is

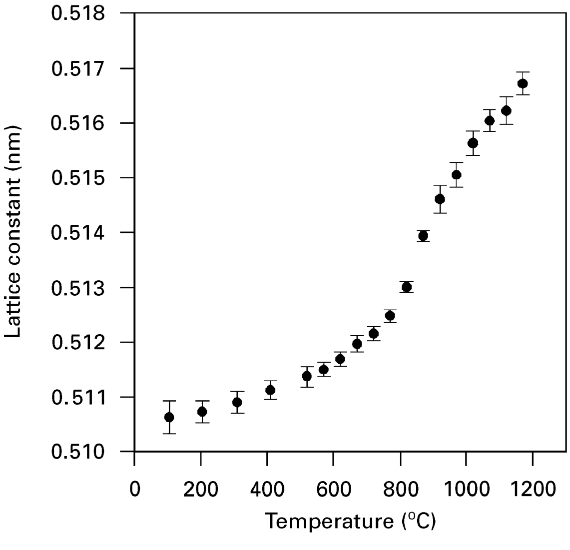

Figure 5 Lattice parameter of the nitrogen-stabilized phase (65 wt % β″) as a function of temperature. The β″ phase was treated as cubic.

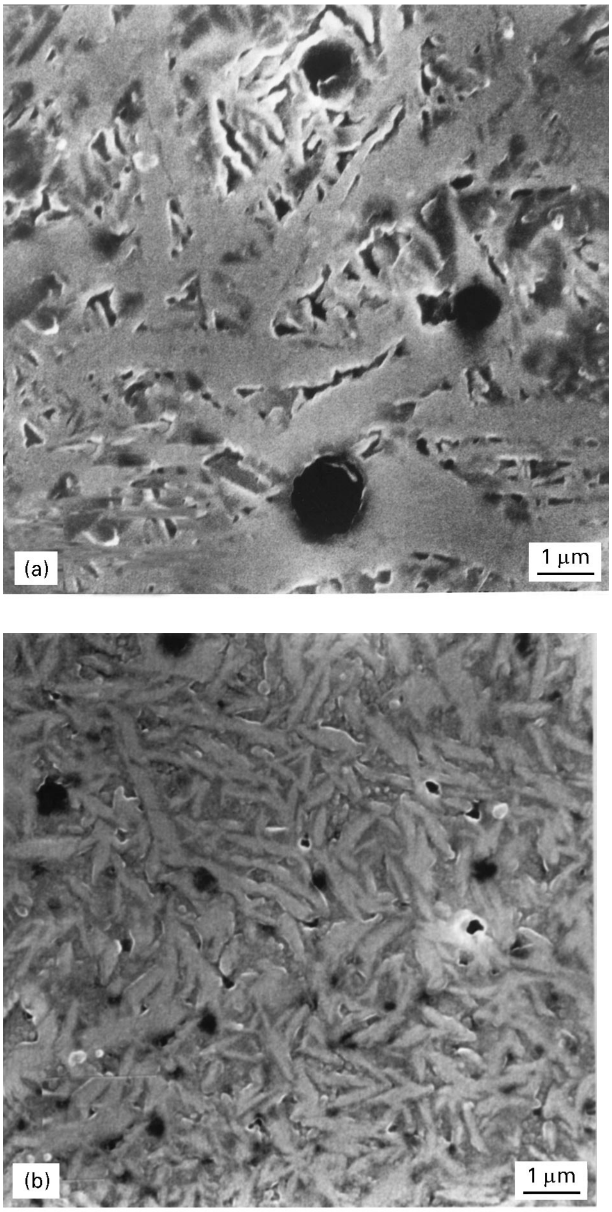

Figure 6 Scanning electron microscope (SEM) image of (a) a slowly cooled and (b) a quenched sample.

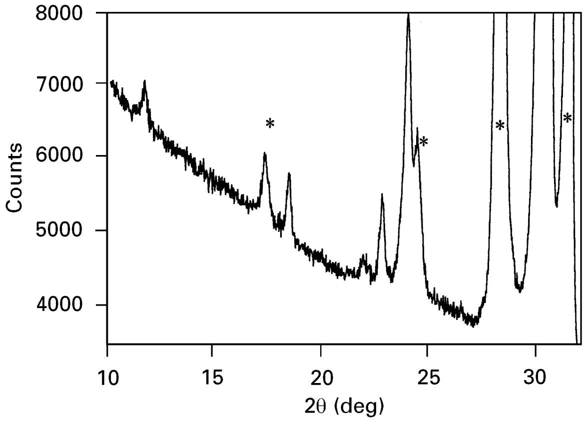

Figure 7 X-ray powder diagram of a β'/m-ZrO_2 sample in the region of small angles. Monoclinic reflections are marked.

insufficient time for the growth of larger ones. A careful X-ray investigation of the quenched sample was carried out, resulting in the determination of a mixture of monoclinic ZrO_2 and β' ($Zr_7O_{11}N_2$). No β'' was observed. Fig. 7 shows the X-ray powder diagram of such a sample in the small-angle region. In comparison with the β'', the observed superlattice reflections are similar, but significantly different. After quenching, the content of the nitrogen-containing phase increased from ~50 to ~77 wt% without a change in the nitrogen content. To understand this behaviour, more information about the crystal structure of β-type phases is necessary. As mentioned in the introduction, anion vacancies are ordered along the trigonal *c*-axis. The crystal structures of all β-type phases can be described by an arrangement of Bevan clusters ($Zr_7O_8N_4$) and Zr_7O_{14} units (Fig. 8). The individual β-type phases differ in the stacking sequence of Bevan clusters and Zr_7O_{14} units along the *c*-axis [14–16]. For example, one Bevan cluster is followed by one Zr_7O_{14} unit in the case of β'. The observed average sequence for β'' phase is approximately four Bevan clusters and one Zr_7O_{14} unit. These special arrangements lead to the given compositions. Quenching the homogeneous high-temperature phases with randomly distributed anion vacancies leads to the formation of a mixture of monoclinic ZrO_2 and the β-type phase with the lowest nitrogen content (β'-$Zr_7O_{11}N_2$), because the reaction is controlled by diffusion. Longer cooling times (e.g. 3 h) allow the formation of β'', which was also found when the sample was cooled down over 3 days. For extremely long annealing times, a mixture of m-ZrO_2 and β phase ($Zr_7O_8N_4$) should be expected. Thus, for the described sample consisting of ~ 50 wt% β'' an increased amount of nitrogen-containing phase after quenching is evident. This is shown by the following calculation.

$$\begin{array}{ll} \multicolumn{2}{l}{Zr_7O_{11.8}N_{1.50}\ \text{(composition of the high-temperature phase)}} \\ \downarrow & \downarrow \\ 0.75Zr_7O_{11}N_2(\beta') & 0.5Zr_7O_{9.5}N_{3.0}(\beta'') \\ +\ 0.25Zr_7O_{14} & +\ 0.5Zr_7O_{14} \\ \text{(quenching)} & \text{(slow cooling)} \end{array}$$

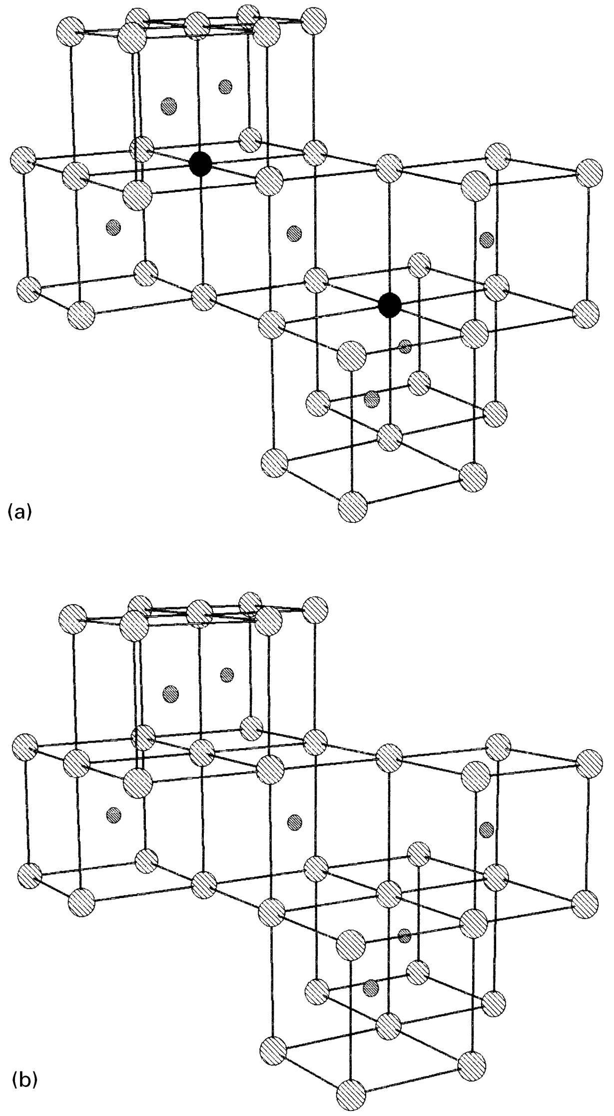

Figure 8 Structure plots of (a) a Bevan cluster ($Zr_7O_8N_4$) and (b) a Zr_7O_{14} unit. Zirconium ions are plotted as small spheres, anions as large light spheres, and vacancies as large dark spheres.

The calculated data are in good agreement with the experimental results.

Such quenched and the corresponding slowly cooled samples were investigated using the described high-temperature X-ray method. The 2θ region between 25° and 34° is shown in Fig. 9. Fig. 10 presents the amount of β' and β'' as a function of temperature. The curve for β'' shows the usual behaviour with a strong increase of X_S (content of stabilized phase) in the region of the phase transition. However, the X_S value decreases slightly at nearly 700 °C, which is probably an indication for a certain solubility of nitrogen in monoclinic ZrO_2. At ~600 °C, the metastable β' phase reacts to β'' phase and m-ZrO_2; the intensities of the m-ZrO_2 reflections increase. Oxygen and nitrogen ions are mobile enough at this temperature for a fast reaction. Thus, the curves are nearly identical in the temperature range above 700 °C.

Another feature of technical interest is the total volume change of the samples during the phase transition. The cell volume of, for example, the cubic high-temperature phase depends on the concentration

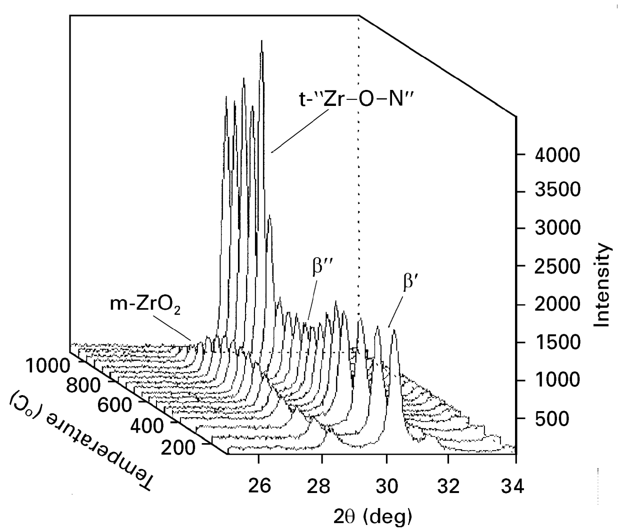

Figure 9 High-temperature X-ray powder diagrams of a quenched sample. β′ reacts to give β″ and m-ZrO$_2$ at nearly 600 °C.

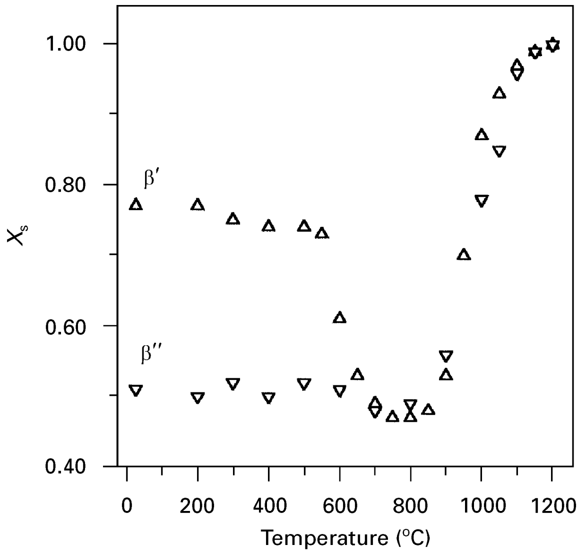

Figure 10 The content of nitrogen-containing phase, X_S, (β″, β′, high-temperature phase) as a function of temperature.

TABLE I Total volume change (calculated) in the temperature range between 800 °C (coexistence of β″/m-ZrO$_2$) and 1100 °C (existence of the high-temperature phases) of some β″/m-ZrO$_2$ samples

β″ (wt %)	ZrN$_{4/3}$ (mol %)	$\frac{V_{1100\,°C} - V_{800\,°C}}{V_{800\,°C}} \times 100$
0	0	− 1.9
10	3.43	− 1.6
20	6.86	− 1.2
30	10.3	− 0.9
40	13.7	− 0.5
50	17.2	− 0.1
60	20.6	+ 0.2
70	24.0	+ 0.5
80	27.4	+ 0.9
90	30.9	+ 1.3
100	34.3	+ 1.7

of nitrogen, which is determined by the ratio m-ZrO$_2$/β″ at ambient temperature. An increase in the nitrogen content leads to a decrease of the cell volume. Table I gives some examples for the total volume change between 800 and 1100 °C. Calculations for different compositions were made using the data (extrapolated in some cases) of Fig. 4. Depending on the composition of the β″/m-ZrO$_2$ samples, the total volume change in the temperature range of the phase transition varies between negative and positive values. A mean thermal expansion of zero was calculated for a sample consisting of an equal mixture of β″ phase and monoclinic ZrO$_2$.

4. Conclusions

1. Anion vacancies play an important role in zirconia systems. The high-temperature behaviour of cation-stabilized zirconia (e.g. with Y$_2$O$_3$) is very similar to that of nitrogen-containing ZrO$_2$. The formation method seems to be insignificant.
2. Cooling samples from temperatures above 1000 °C leads to the formation of β-type phases with ordered anion vacancies in the ZrO$_2$–Zr$_3$N$_4$ system. Depending on the cooling rate, different zirconium oxynitride phases are observed.
3. The volume change of β″/m-ZrO$_2$ samples during the phase transition depends strongly on composition. Calculations point to the fact that it is possible to produce samples with positive, negative, or without a mean thermal expansion in the temperature range between 800 and 1100 °C.

Acknowledgements

The authors thanks Mr J. Wrba for experimental help, and Professor G. Müller for financial support. This work was also supported by the Deutsche Forschungsgemeinschaft (DFG), under Grant no. Le 781/2-1.

References

1. V. S. STUBICAN, "Advances in Ceramics", Vol. 24, "Science and Technology of Zirconia III", edited by S. Somiya, N. Yamamoto, H. Yanagida (The American Ceramic Society, Westerville, 1988) p. 71.
2. P. DUWEZ, F. ODELL and F. H. BROWN, *J. Am. Ceram. Soc.* **35** (1952) 107.
3. C. F. GRAIN, *ibid.* **50** (1967) 288.
4. V. S. STUBICAN and S. P. RAY, *ibid.* **60** (1977) 534.
5. H. G. SCOTT, *J. Mater. Sci.* **72** (1977) 311.
6. V. S. STUBICAN, R. C. HINK and S. P. RAY, *J. Am. Ceram. Soc.* **61** (1978) 17.
7. J. R. HELLMANN and V. S. STUBICAN, *ibid.* **66** (1983) 260.
8. C. PASCUAL and P. DURAN, *ibid.* **66** (1983) 23.
9. J. C. GILLES, *Bull. Soc. Chim. Fr.* **22** (1962) 2118.
10. R. COLLONGUES, J. C. GILLES, A. M. LEJUS, M. PEREZ, Y JORBA and D. MICHEL, *Mater. Res. Bull.* **2** (1967) 837.
11. Y. B. CHENG and D. P. THOMPSON, *Special Ceram.* **9** (1992) 149.
12. *Idem, J. Am. Ceram. Soc.* **76** (1993) 683.
13. M. LERCH, *ibid.*, in press.
14. M. LERCH, F. KRUMEICH, and R. HOCK, in "Transformation Kinetics and Reactivity of Solids", edited by P. Grange *et al.*, Louvain-la-Neuve, (1995) p. 123.

15. R. HOCK, M. LERCH, K. S. KNIGHT and H. BOYSEN, *Z. Kristallogr. Suppl.* **9** (1995) 298.
16. M. LERCH, R. HOCK and E. FÜGLEIN, *ibid.* **9** (1995) 193.
17. M. LERCH, L. JACOBSEN and G. MÜLLER, *ibid.* **8** (1994) 256.
18. R. C. GARVIE and P. S. NICHOLSON, *J. Am. Ceram. Soc.* **55** (1972) 303.
19. M. LERCH, D. WALTER, O. RAHÄUSER, W. LAQUA and K. S. KNIGHT, *Z. Kristallogr. Suppl.* **9** (1995) 305.
20. M. YASHIMA, S. SASAKI, M. KAKIHANA, Y. YAMAGUCHI, H. ARASHI and M. YOSHIMURA, *Acta Crystallogr.* **B50** (1994) 663.
21. J. W. ADAMS, H. H. NAKAMURA, R. P. INGEL and R. W. RICE, *J. Am. Ceram. Soc.* **68** (1985) 228.

Received 13 June 1995
and accepted 12 August 1996